Civil Engineering Infrastructures Journal 2025, 58(2): 265-285
DOI: 10.22059/ceij.2024.369144.1990

RESEARCH PAPER

The Free Vibration Characteristics of a Concrete Arch Gravity Dam Using Finite Element Technique

Sougata, M.[1] and Nallasivam, K.[2*]

[1] P.G. Student of Structural Engineering, Department of Civil Engineering, National Institute of Technology (NIT) Hamirpur, Himachal Pradesh, India.
[2] Assistant Professor, Department of Civil Engineering, National Institute of Technology (NIT) Hamirpur, Himachal Pradesh, India.

Received: 4 Dec. 2023; Revised: 21 Mar. 2024; Accepted: 29 May 2024

ABSTRACT: The objective of this study is to ascertain the free vibration analysis of an arch dam, which needs to be identified prior to doing a dynamic analysis of the dam in response to hydrodynamic and seismic loads. This work focuses on analyzing the free vibration analysis of an arch dam under several conditions: dam-soil contact, dam without soil interaction, and dam in a soil-reservoir system. The analysis is conducted using the finite element software ANSYS. This study's findings include an estimation of the natural frequency and mode shape of various dam systems by free vibration analysis. When foundation interaction is taken into account, the dam's natural frequency is found to be lower than that of a dam with fixed support, which is related to a reduction in stiffness and an increase in the vibrating system's mass. This paper focuses exclusively on analyzing the natural vibration of a concrete arch-gravity dam structure. Dam engineers can conduct additional evaluation of this research to enhance the structural effectiveness and functionality of the dam. Additionally, this research can serve as a basis for analyzing the concrete arch-gravity dam's response to different dynamic loads.

Keywords: Concrete Arch Dam, Free Vibration, Eign Value Problem, Modal Analysis, Finite Element Method, FEM ANSYS Model.

1. Introduction

The concrete arch-gravity dams are visually appealing due to their arch action formed between two hills. This unique design presents new challenges in its application for irrigation, cultivation, flood safety, and the generation of renewable energy. These dams can be utilized to promote the growth and sustainability of a nation. The arch dam's design serves a structural purpose by facilitating the redistribution of hydrostatic pressure across the dam. These structural systems are characterized by their geometric complexity, which includes combinations of different external and interior radius or arc angles. Additionally, they include variable and irregular centers for both exterior and interior arches. The vibrational characteristics of these dams can have an impact on their longevity, safety, and livability, as well as resulting in societal, economical, and ecological damages. Therefore, the objective of this work is to determine the natural oscillation behavior of an arch dam, which is crucial to understand prior to doing a dynamic analysis of the dam in response to hydrodynamic and seismic stresses. Yaghin and Hesari (2008) employed the ABAQUS

* Corresponding author E-mail: nallasivam@nith.ac.in

finite element technique software to assess the dynamic properties of arch concrete dams that do not have supports and dams that do not have bedrock support systems.

The temporal evolution of the primary stress, secondary stress, deformation of the dam crest, and river bed level has been computed using the collected data. The maximum values of these parameters during the seismic event have been thoroughly analyzed. Berrabah et al. (2012) conducted a comprehensive modal analysis of the Brezina Arch dam using the Finite Element Method (FEM) and ANSYS software. Three-dimensional (3D) models were created to analyze the impact of the foundation on the arch dam. The models included dams without a soil foundation, dams with soil but no mass, and dams with a soil foundation. Additionally, a study on the phenomenon of damped vibration was conducted. It was determined that the basic frequency of undamped and damped vibrations obtained from a dam with a soil foundation model was much lower than that of a dam without a soil foundation model, and also considerably lower than those obtained from a dam without a soil mass model. The results indicated that any damped vibration ratio was deemed to be lower in value compared to the dam without soil mass and the dam with soil foundation. Furthermore, it was significantly lower than the dam without a soil foundation model. The fundamental frequency of each undamped and damped mode was significantly lower than that of the dam without soil material.

Zhuan-Yun (2014) conducted a study to examine the specific load-bearing properties and seismic behavior of the largest elevated arch dam in a hydroelectric network. They developed a 3D finite element numerical model using ANSYS to analyze the interaction between the arch dam and its foundation. The study focused on static analysis under basic combined effects and dynamic behavior under key factors that contribute to the behavior of the elevated arch dam. The initial order had a frequency of 3.34 Hz, and its vibrating mode was determined by the orientation along the river, as revealed by the examination of the vibrating characteristics of the elevated arch dam using the Lanczos method. The dam's planned system was deemed appropriate and reliable as the largest dynamic deformation and earthquake stress remain below the required limitations.

Patil and Awari (2015) investigated the impact of soil interaction on gravity dams by employing the finite element analysis program ANSYS. The analysis revealed that when taking into account soil stiffness and mass, the displacement of a dam with a soil foundation contact is greater than that of a dam without such an interface. Khosravi and Heydari (2015) utilized the finite element program ANSYS to ascertain the most advantageous configuration of concrete gravity dams, while also considering the interaction between the dam, water, and foundation rock. A two-dimensional (2D) finite element model comprising the dam, reservoir, and base was available. The dam was considered in four different modeling scenarios: a) Dam with a fixed foundation and an empty reservoir; b) Dam with a flexible foundation and an empty reservoir; c) Dam with a fully functional reservoir and a stable foundation; and d) A reservoir dam with a pliable foundation is required. A study was conducted on the modal characteristics and mode shapes of the Pine Flat, Koyna, and modelled triangular dams. The results were then compared to existing reference data in order to assess the accuracy and reliability of this modeling approach. The numerical findings confirmed the effectiveness of the suggested method for simulating the geometry of gravity dams. It was acknowledged that the inclusion of the dam-water-foundation-rock interaction is crucial in order to build a secure gravity dam.

Varughese and Nikithan (2016) utilized the finite element software ANSYS to assess the static, modal, and transient

analyses of the dam reservoir-foundation system. The reservoir was simulated using the FLUID 29 fluid acoustic element, while the dam and foundation were simulated using the PLANE 42 2D planar strain element. This combination accurately captured the fluid-structure interaction. A formulation for the fundamental period of concrete dams was established using modal analysis.

Pandey et al. (2016) conducted a comparative analysis between 3D and 2D models of a monolith gravity dam using ANSYS software. The researchers determined that a modal analysis can accurately determine the attendance for out-of-plane frequency by studying 3D models, which 2D models may not accurately depict. Consequently, the 3D models exhibited higher levels of stress in comparison to the 2D models when analyzing loads. The 3D model experienced higher tensile strains at the heel of the shorter cross-section due to hydrostatic loads.

Altunişik et al. (2016) investigated the impact of reservoir water on the vibration properties of a model arch dam, both before and after reinforcement. A model of an arch dam-reservoir-foundation was created for the purpose of this experiment. Experiments were conducted on arch dam models, both demolished and strengthened, to study the impact of water on the dynamic characteristics. These experiments involved analyzing ambient vibrations in both unoccupied and filled reservoir conditions. The dynamic properties were acquired by an improved frequency domain decomposition method. Afterwards, the dynamic characteristics obtained from the damaged and reinforced dam models were compared. The study also examined the natural frequencies of both damaged and strengthened models to determine if the impact of strengthening on the frequencies is detectable.

Esmaielzadeh et al. (2019) conducted research to detect and determine the extent, location, and elevation of any structural harm to the dam. Three finite element models of the Pine Flat, Bluestone, and Folsom dams were selected as case studies to achieve these objectives. The dams were modeled using SAP2000 software to analyze their geometric, physical, and mechanical characteristics in both undamaged and damaged conditions. Multiple modal inquiries determined the frequencies and configurations of the structural movements.

Messaad et al. (2021) conducted a modeling study to analyze the occurrence of dam reservoir-foundation coupling, taking into account the presence of both the reservoir and the foundation. This approach allowed for a more accurate assessment of the overall performance of the system. The study utilized the ANSYS FEM to examine the dynamic properties of a dam-reservoir foundation system when subjected to seismic forces.

Verma and Nallasivam (2020, 2021a,b) conducted a study on the static and free vibration analysis of box-girder bridges. Hariri-Ardebili et al. (2021) performed a sensitivity study on dams using a hybrid surrogate model that combines Random Field (RF) and Polynomial Chaos Expansion (PCE). The results illustrated the dam's free vibration characteristics using natural frequencies and mode shapes.

Hariri-Ardebili et al. (2016) conducted a parametric research on a concrete gravity dam using finite element analysis. The researchers determined that the primary causes of failure for these dams were cracking, overturning, and sliding. Additionally, they found that the vibration characteristics of the dams were primarily influenced by the first six modes.

Amini et al. (2021) conducted a sensitivity study on aging concrete gravity dams using Kriging and PCK meta-models. It was discovered that these models were efficient in conducting reliability analysis while reducing computing time.

Abdollahi et al. (2022) highlighted the increasing requirement for a comprehensive dam form design framework that considers

uncertainties and can handle many hazards. This framework should also incorporate time-dependent demand and capacity models. The technique was employed to optimize the configuration of gravity dams by utilizing a collection of time-varying and time-invariant performance indicators at both the local and global scales. Ultimately, the framework was expanded to encompass a versatile dam class that incorporates different heights, strengths of concrete, and flexibility from the base to the concrete structure.

Li et al. (2022) conducted a study on the interaction of dams, water, and foundation rocks in a complicated layered half-space. A novel Scaled Boundary Finite Element Method (SBFEM) was devised for the purpose of examining the interaction between a 3D dam and its foundation. The foundation rock was represented by three unique models: A homogeneous half-space, a horizontal layered half-space, and an inclined half-space.

Rasa et al. (2024a) proposed a computational model that efficiently examined the seismic behavior of concrete gravity dams using the Laplace domain-FEM methodology. The study findings suggested that longer periods of large earthquakes were linked to greater deformations, stress fluctuations, and an increased probability of damage to the dam structure.

Rasa et al. (2024b) examined the dynamic reactions of a concrete machine foundation when subjected to impact loads. The study also considered the deterioration of concrete due to chemical and mechanical processes over time. The deterioration of concrete over time significantly affected the dynamic reactions of machine foundations. There was a direct relationship between the severity of high stress responses at the foundation and the rate at which concrete deteriorates. Machine foundations built on medium soil types exhibited a reduction of 32.6% in stress responses between the ages of 0 and 50 years.

Sharma and Nallasivam (2023) utilized the ANSYS program, a commercial finite element software, to compute the static response of a 2D model of the Bhakra concrete dam. Several 2D models were created to represent different types of dams, including those with a solid basis, as well as those with a foundation that had mass and those with a foundation that was weightless.

Rasa et al. (2024c) examined the dynamic behavior of the interaction problem between aging concrete gravity dams and reservoirs. Due to concrete deterioration, the dam undergoes elongation in its lifespan, resulting in dynamic responses such as horizontal and vertical displacements, as well as changes in its basic periods. This elongation ultimately resulted in a reduction in the seismic stability of the dam.

Rasa et al. (2024d) presented a dam-reservoir interaction model that integrates many parameters like water compressibility, surface water sloshing, and radiation damping at the far-end reservoir. The purpose of this model was to analyze the influence of concrete degradation on the seismic response and effectiveness of gravity dams. The deterioration of concrete was assumed to take place due to both mechanical and chemical processes over the whole lifespan of the dam.

Hashempour et al. (2023) proposed a simplified nonlinear model to analyze earthquake effects on concrete arch dams. It captureed concrete's behaviour under load changes better than complex models. The model accurately predicted crack patterns and final strength. The analysis of the Morrow Point dam considered dam-water interaction and used two damping algorithms. The research suggested that this efficient model can replace complex ones while highlighting the importance of choosing appropriate damping for accurate results.

Heshmati et al. (2013) compared stress and strain methods for evaluating arch dam seismic response. A detailed dam model considered interaction with the reservoir and foundation. While both stress and strain

(cumulative inelastic strain) were analyzed and showed some correlation, the paper argued that the strain-based method provided a more refined picture of dam damage. This potentially leads to different conclusions about dam safety compared to relying solely on stress analysis. In essence, the paper suggested strain-based methods offer a more nuanced approach to dam safety assessments.

Rezaiee-Pajand et al. (2023) proposed a novel method for analyzing vibrations in concrete dams. The traditional approach was computationally expensive due to a complex problem type. They introduced a new strategy that avoids this issue. They formulated two new, easier-to-solve eigenvalue problems and claimed their method was more accurate than existing techniques. The paper validated this with tests on benchmark dams. While the details of the method and the extent of accuracy improvement were not provided here, this new approach had the potential to improve efficiency and accuracy in dam vibration analysis significantly.

Tavakoli et al. (2023) addressed a vulnerability in Roller-Compacted Concrete (RCD) dams: thermal cracks stemming from cement variations. These cracks can worsen during earthquakes. The study examined this phenomenon by utilizing a 3D FEM constructed in the ABAQUS program. The model considered both translational and rotational earthquake motions to analyze crack propagation. Results showed that existing cracks significantly propagated during earthquakes, with rotational motion playing a crucial role. It could increase crack propagation energy by up to 50% for some earthquakes. This highlighted the importance of considering both crack presence and rotational motion for improved earthquake safety assessments of RCD dams.

According to the literature reviews, most researchers have performed both closed-form solution and non-closed-form-based free vibration analysis of the concrete gravity dam system. In addition, a small number of researchers have performed parametric studies on the free vibration characteristics of several types of concrete gravity dam systems. The objective of this work is to develop a 3D FEM using ANSYS software to examine the free vibration properties of the concrete gravity dam system, with a focus on natural frequencies and mode shapes. The model's reliability is validated using mesh convergence analysis and comparison with findings from prior researchers' investigations. Several parametric experiments are conducted to examine the free vibration properties of concrete gravity dams. The study's findings are crucial for dam engineers as they provide significant insights to enhance their comprehension of the modal features of a concrete gravity dam. Engineers will benefit from this knowledge as it will assist them in studying the dynamic behavior of concrete gravity dams caused by hydrodynamic and earthquake loads.

2. Materials and Methods

2.1. Finite Element Modelling of Concrete Arch Gravity Dam System

Figure 1 depicts the sequential steps for assessing a FEM model of a concrete arch gravity dam system.

2.2. Modelling of a Concrete Arch-Gravity Dam

2.2.1. Dimensional Configurations of The Dam

Table 1 presents the configuration variables of the dam, whereas Figure 2 illustrates the cross-section of the dam using these geometry variables.

This study examines the proposed construction of a concrete arch-gravity dam proposal at Jankar Jangal, located near Chamba, Himachal Pradesh, India, in the Ravi riverbed basin.

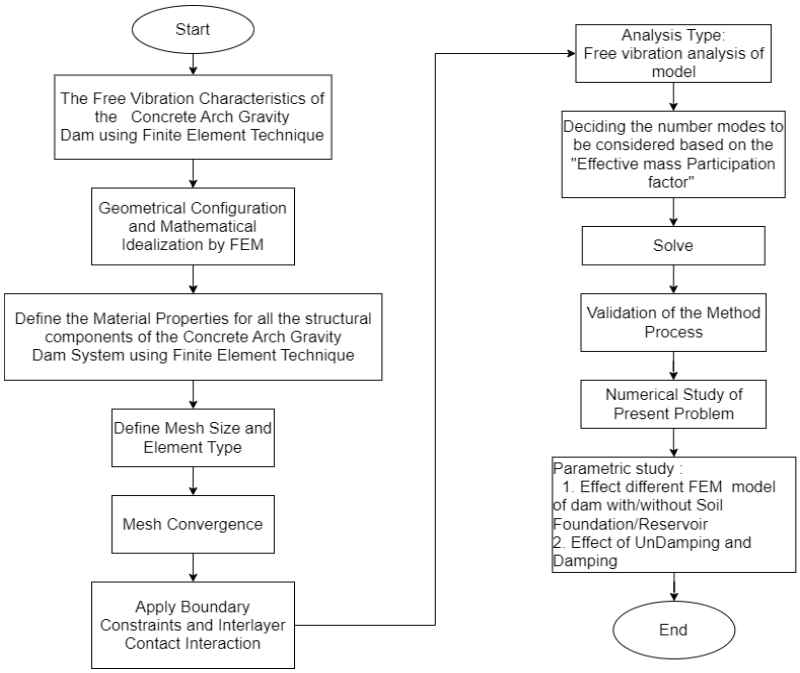

Fig. 1. The schematic sequence used to calibrate the FEM model

Table 1. The parameters of the geometry of the dam

	Model category	Concrete arch-gravity dam (m)
Concrete dam	Width(at Crest Level)	4
	Width(at foundation level)	36.3
	Height	25.94
	Curve span	20.05
	Max water depth	25.44
Foundation	Model category	Soil layer in m
	x	27
	y	48.3
	z	95

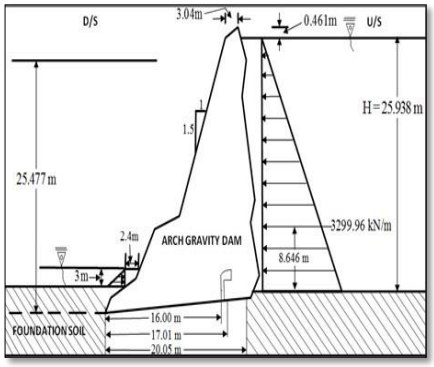

Fig. 2. Geometry configuration of the dam

2.2.2. Concrete Arch-Gravity Dam Mathematical Idealization Using Finite Element Modelling

The FEM has become an indispensable tool for computationally addressing a diverse range of technical problems. The finite element-based software (Zhang et al., 2013; ANSYS Manual, 2019; Tickoo, 2021) was utilized to model the concrete arch-gravity dam in this study. Figures 3-5 display the three distinct methods of discretizing the dam model. In order to examine the modal behavior of the dam, three distinct model situations are selected as follows: Model 1 refers to a dam that has a fixed support and does not have a soil base. The reservoir associated with this dam is called "fixed-empty" and is seen in Figure 3. Model 2 refers to a dam that has a dirt base and an empty reservoir. This particular model is called "mass-empty" and may be seen in Figure 4. Model 3 refers to a dam that has a soil foundation and a reservoir that is completely filled with water. This particular dam is known as the "mass-fluid" dam, as seen in Figure 5. For Model 1, the dam is considered as a fixed boundary constraint at the base.

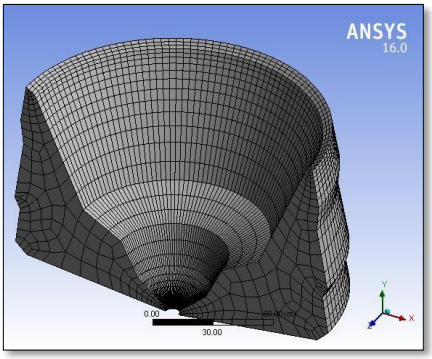

Fig. 3. Dam with a fixed support and does not have a soil base

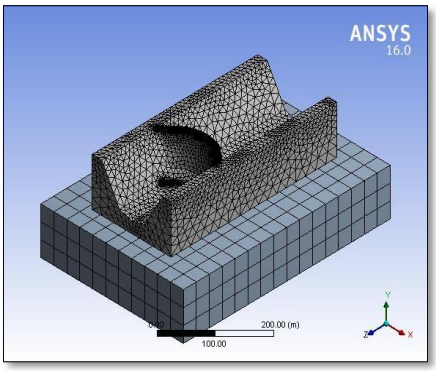

Fig. 4. Dam with a dirt base and an empty reservoir

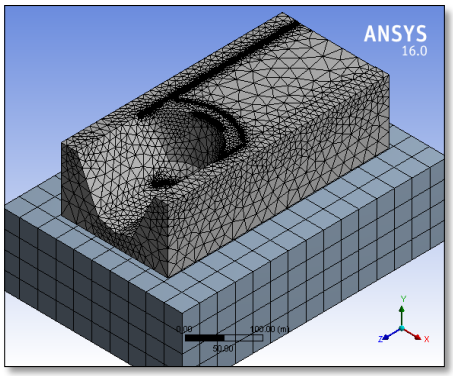

Fig. 5. Dam with a soil foundation and a reservoir that is completely filled with water

In Models 2 and 3, the dam is fixed at the base of the foundation. The length of the reservoir is determined by multiplying the depth by a factor of 1.5. The dam has undergone a comprehensive 3D analysis. The implementation of ANSYS was utilized for the purpose of modeling and analysis. The dam, soil base, and reservoir have all been created with 3D solid components. Each node of an element possesses six degrees of freedom, encompassing translations and rotations along the x, y, and z axes.

2.3. Material Properties

Table 2 provides the characteristics of the material for the base soil of a concrete arch dam and the water in the reservoir. Multiple organizations provide specific guidelines for ensuring safe construction.

The concrete mass is regarded as homogeneous, isotropic, and elastic. An ideal foundation soil is a uniform, equally responsive, and flexible medium. Herein, the Viscous damping of the structure is assumed to be Rayleigh damping form (Chopra, 2007). In this parametric investigation, the classical viscous damping ratio will be varied at 2%, 5%, and 10%.

2.4. Element Type and Meshing

Figure 6 illustrates the SOLID186 elements, which are 3D solid elements with 20 nodes and exhibit quadratic displacement behavior. Meshing is a crucial component in a finite element model. Using finer meshes in the FEM model can yield more accurate outcomes, but it also results in a larger number of elements and nodes, which in turn leads to higher computational costs. Choosing the optimal element size is critical since it directly affects the trade-off between computational expense and solution precision.

Table 2. Material properties of the concrete dam, reservoir water, and foundation soil

Concrete dam	The mass density of concrete ρ (kg/m^3)	2500
	Modulus of elasticity of concrete E (MPa)	28500
	Poisson's ratio (μ)	0.2
Reservoir water	Density of water (kg/m^3)	1000
	Bulk modulus of elasticity of water K (MPa)	2020
	Sonic velocity or Speed of pressure wave (m/s)	14500
	Wave reflection coefficient	0.25
Foundation soil	The mass density of foundation Soil ρ (kg/m^3)	2100
	Modulus of elasticity of foundation soil E (MPa)	14500
	Poisson's ratio μ	0.25

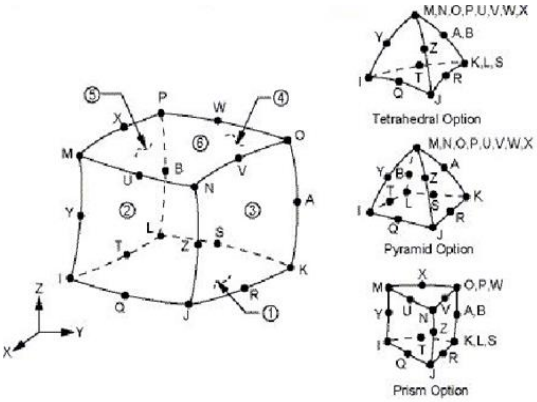

Fig. 6. Multiple sorts of elements utilized to model different components of a concrete arch-gravity dam

The ANSYS Manual (2019) is a robust FEM tool that offers users the ability to define and adjust element sizes according to the specific characteristics of the investigated model or system. The choice of element size and suitable meshing procedures is a critical determinant in ensuring the accuracy and efficiency of simulations conducted using software like ANSYS in the domain of FEM. The characteristics of the element type and meshing size employed for different components of the current model are described in Table 3.

Table 3. Types of elements and meshing size (ANSYS manual, 2019)

Components	Mesh size (mm)	Element type
Concrete dam	250	3D Solid 186
Soil foundation	300	3D Solid 186
Reservoir water	300	3D Solid 186

A denser mesh with a greater number of smaller pieces typically produces more precise outcomes, particularly in regions with intricate geometry, as depicted in Figures 3-5.

2.5. Boundary Conditions

When creating a finite element model, the selection of boundary conditions is crucial. It is vital to choose appropriate boundary conditions in order to accurately produce meaningful results. The boundary condition for the structure, as indicated in Table 4, may be categorized into two primary parts: internal boundary conditions, which involve the interaction between each component, and outer boundary conditions, which involve the interaction with the external environment.

Table 4. Boundary conditions (Berrabah et al., 2012)

Components	Boundary condition	
Model-1	Fixed boundary constraints at the base of the dam and the side of the dam	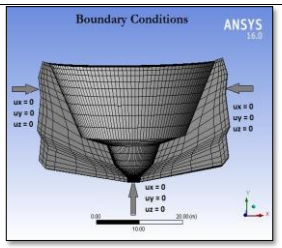
Model-2	Fixed boundary constraint at the base of the foundation and side of the dam, and bonded boundary constraint between the interface of the dam and foundation	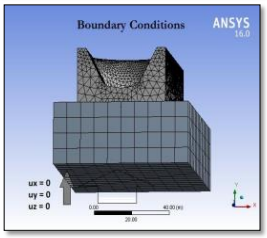
Model-3	Fixed boundary constraint at the base of the foundation and side of the dam, and bonded boundary constraint between the interface of the dam and foundation	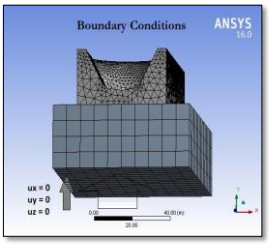

Regarding the outer boundary condition, it is important to note that the bottom and four sides of the foundation were simulated with fixed conditions, meaning that all degrees of freedom were restrained. The internal boundary condition was established by implementing a bonded interaction requirement between the interface of the dam and foundation.

2.6. Modal Analysis of Concrete Gravity Dam System

A frequently utilized technique in the field of structural dynamics is the mode superposition approach. This approach enables the analysis of various dynamic loads acting on structures, including both transient and steady-state responses. Modal frequencies and modal vectors of a structure are usually calculated in the absence of dampening. The hypothesis put forth by Borino and Muscolin (1986) posits that the precise frequencies of structures, commonly referred to as damped frequencies, demonstrate a negligible departure from their un-damped counterparts. The elucidation of the topic is efficiently achieved by employing illustrative situations (Rasa and Budak, 2021).

2.6.1. Un-Damped Modal Analysis

Before doing dynamic analysis, it is essential to carry out free vibration analysis to ascertain the inherent dynamic characteristics of the model structure. Free vibration refers to the phenomenon of vibrations occurring at the inherent frequency of a system without any external influence or interference. The utilization of mode analysis allows for a thorough depiction of the dynamic properties of a vibrating system, encompassing its mode shapes and inherent frequency. The equation of motion for an undamped free vibration system is dictated by the overall structural system, which includes the cross-section, materials utilized, and other important aspects. These parameters collectively govern the fundamental frequencies and mode shapes of the vibration equation.

$$[M]\left[\ddot{\delta}\right] + [K][\delta] = 0 \quad (1)$$

where $[M]$: is global mass matrix, $\left[\ddot{\delta}\right]$: is global acceleration matrix, $[K]$: is global stiffness matrix, and $[\delta]$: is global displacement matrix. When analyzing the un-damped free vibration, it can be assumed that the motion follows a harmonic pattern in its natural mode. Therefore, the reaction is depicted as follows:

$$[\delta] = [X]\sin(\omega t + \emptyset) \quad (2)$$

where $\{X\}$: is nodal amplitude of vibration, ω: is angular natural frequency (rad/sec), and ϕ: is phase angle. From Eqs. (1) and (2), a generalized eigenvalue problem can be obtained (Eq. (3)).

$$\left[[K] - \omega^2[M]\right][X] = 0 \quad (3)$$

When solving Eq. (3), a standard Eigen solver is utilized to ascertain the inherent frequency and mode shapes of the structures. To get the dam's dynamic characteristics, the equation (Clough and Penzien, 1995) is solved using an ordinary eigen solver. The theoretical natural frequency, as mentioned in Clough and Penzien (1995), can be written as Eq. (4).

$$f_n = n^2\pi^2\sqrt{\frac{EI}{mL^4}}n \quad (4)$$
$$= 1.2.3. \ldots$$

where f_n: is the frequency of each order, EI: is the flexural stiffness of the cross-section, m: is mass per unit length, and L: is the length of the beam. The corresponding mode shape, $\emptyset_n$, can be written as Eq. (5).

$$\emptyset_n(x) = C_1\sin\frac{n\pi x}{L} \quad (5)$$

2.6.2. Damped Modal Analysis (Yaghin and Hesari, 2008; Berrabah et al., 2012)

Damping is a phenomenon that affects

every dynamic process in nature. The existence of an utterly undamped vibration is not observed in actuality. ANSYS offers multiple options for simulating the impact of structural damping. In the context of modal analysis, it is possible to employ both Rayleigh damping and material-dependent damping techniques. In addition, distinct dampening components can be utilized. The two eigen solvers that can be utilized for this objective are the Damped Method and the QR-Damped method. Recall that the equations of free-damped vibration are as Eq. (6).

$$[M][\ddot{x}]+[C][\dot{x}]+[K][x]=0 \tag{6}$$

where [M], $[C]$ and [K] are the global mass, damping and stiffness matrix, $[\ddot{x}]$,$[\dot{x}]$ and $[x]$: are the global acceleration, velocity and displacement matrix.

In this case, it is assumed that the dam's viscous damping follows the Rayleigh damping form, as described by Chopra (2007). The damping matrix in this scenario is regarded as being proportional to either the mass or the stiffness matrix, or a combination of both. This is because the undamped mode forms are orthogonal for each of these factors, as indicated by the following equations.

$$[c]=\alpha[m]+\beta[k] \tag{7}$$

It is also known as Rayleigh damping. Rayleigh damping determines the relationship between the damping ratio and frequency.

$$\xi_n=\frac{\alpha}{2\omega_n}+\frac{\beta\omega_n}{2} \tag{8}$$

The proportionality constants α and β have units of seconds to the power of negative one and seconds, respectively. The terms "mass proportional damping constant" and "stiffness proportional damping constant" are used to refer to these concepts. If the damping ratio ξ_m, ξ_n associated with two frequencies in the m^{th} and n^{th} modes is known, the two damping factors can be determined by solving a pair of simultaneous equations. By substituting Eq. (8) into the equations for each of these two examples and representing the resulting equations in matrix form, Eq. (9) is obtained.

$$\begin{Bmatrix}\xi_m\\ \xi_n\end{Bmatrix} = \frac{1}{2}\begin{bmatrix}1/\omega_m & \omega_m\\ 1/\omega_n & \omega_n\end{bmatrix}\begin{Bmatrix}\alpha\\ \beta\end{Bmatrix} \tag{9}$$

If the damping coefficients of the two modes are equal, the $(\xi = \xi_m = \xi_n)$ solution of the simultaneous equations leads to Eq. (10).

$$\begin{Bmatrix}\alpha\\ \beta\end{Bmatrix} = \frac{2\xi}{\omega_m+\omega_n}\begin{bmatrix}\omega_m\omega_n\\ 1\end{bmatrix} \tag{10}$$

According to ANSYS (2019), alpha damping, also known as mass damping, may be disregarded in numerous practical structural issues when the value of ($\alpha = 0$) is equal to zero. This disregard is typically observed in bodies that exhibit resistance to wind or in undersea applications. In such instances, one of the proportionality constants value (β) can be assessed based on the known value of damping and frequency, ξ_i *and* ω_i, as follows.

$$\xi_i \text{ and } \omega_i, \text{ as: } \beta=\frac{2\xi_i}{\omega_i} \tag{11}$$

In Eq. (11), the damping ratio (ξ) is assumed to be 2%, 5%, and 10%.

3. Results and Discussion

3.1. Free Vibration Characteristics of a Concrete Arch-Gravity Dam

The response time of a structure is affected by the ratio of force-frequency (ϖ) resulting from outside loads such as live loads and seismic forces, to the inherent frequency (ω) of the structure in relation to its weight. The natural frequencies align with the force frequency, which may result

in resonance and cause structural harm.

3.1.1. Validation of the Method

The modal analysis results for the first five modes of the current work's concrete arch-gravity dam have been confirmed by the study conducted by Berrabah et al. (2012). The validity of this analysis regarding the dam problem, considering both the presence and absence of soil-structure interaction, is confirmed by comparing it with ANSYS results obtained from simplified analyses of the fundamental mode response. The solid 186 elements were employed to replicate the behavior of the concrete arch-gravity dam. The concrete arch-gravity dam was meshed with a mesh size of 200 mm. The numerical problem at hand involves a concrete arch-gravity dam with specific geometric dimensions. The problem focuses on the material properties, element types, and boundary conditions of different components of the dam, as outlined in Tables 1-4.

By utilizing ANSYS software, the outcomes of prior research publications are juxtaposed with the findings of the present study, as depicted in Figure 7. Given the strong concurrence between the current findings and the established results in existing literature, the methodology employed in this study is deemed suitable for addressing the dam-soil interaction phenomenon and accurately determining the fundamental natural frequency.

3.1.2. Present Problem

Several modal analyses were performed to determine the fundamental natural frequency range of the concrete arch-gravity dam, as depicted in Figures 3-5. The solid 186 elements were employed to replicate the behavior of the concrete arch-gravity dam. The concrete arch-gravity dam was meshed with a mesh size of 400 mm.

The numerical problem at hand concerns a concrete arch-gravity dam with specific geometric dimensions. It involves analyzing the material properties, element types, and boundary conditions of different components of the dam, as outlined in Tables 1-4. An arch dam was subjected to modal analysis in order to ascertain the primary frequencies and mode configurations of the dam construction. The modal frequencies and dynamic responsiveness of gravity dams during earthquakes are influenced by the foundation and water reservoir. An eigenvalue analysis is conducted on the three models mentioned above, and a comparative examination of the modal frequencies is presented in Figures 8-10.

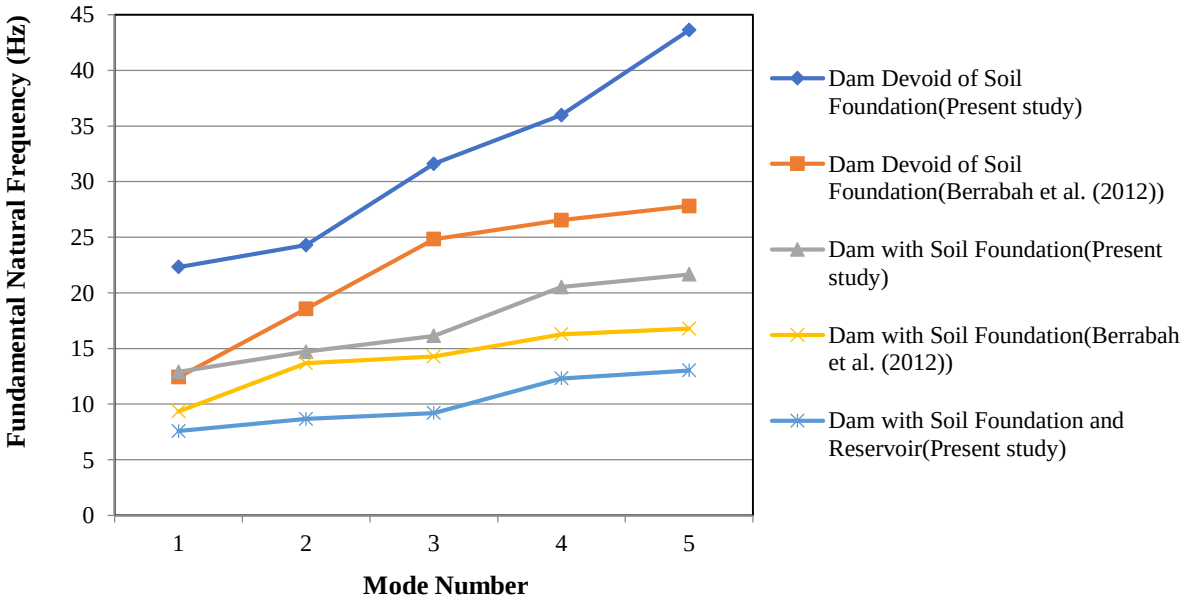

Fig. 7. Frequency of first five modes for undamped free vibration compared with Berrabah et al. (2012) results

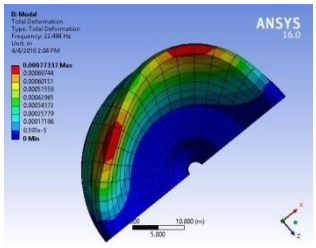

(a) Mode 1 (1st mode of longitudinal DOF) 22.323 Hz (displacement) 1.08%

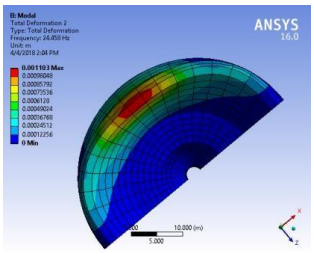

(b) Mode 2 (1st mode of lateral DOF) 24.288 Hz (displacement) 1.63%

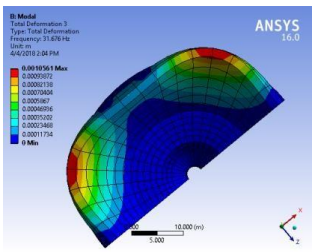

(c) Mode 3 (1st mode of torsional DOF) 31.597 Hz, 1.13%

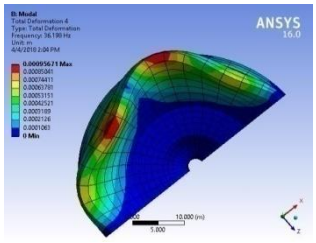

(d) Mode 4 (2nd mode of longitudinal DOF) 35.978 Hz (displacement) 1.26%

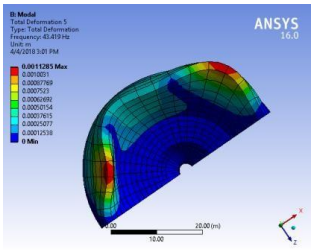

(e) Mode 5 (2nd mode of lateral DOF) 43.609 Hz (bending and torsion) 1.24%

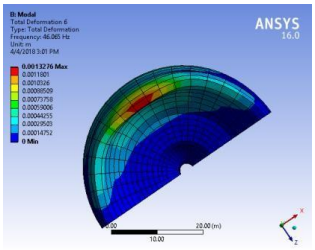

(f) Mode 6 (2nd mode of torsional DOF) 47.472 Hz (displacement) 1.61%

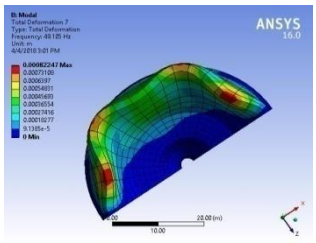

(g) Mode 7 (3rd mode of lateral DOF) 49.018 Hz (bending) 1.33%

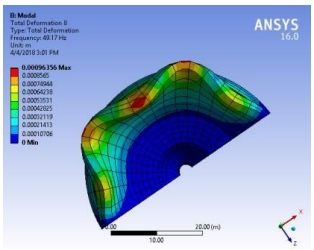

(h) Mode 8 (3rd mode of longitudinal DOF) 49.596 Hz (bending) 1.29%

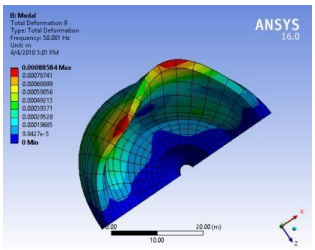

(i) Mode 9 (3rd mode of torsional DOF) 51.503 Hz (torsional) 1.74%

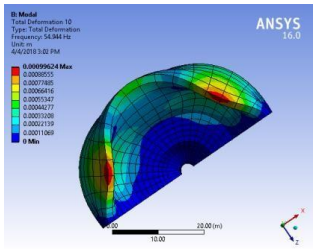

(j) Mode 10 (4th mode of longitudinal DOF) 55.643 Hz (bending) 1.20%

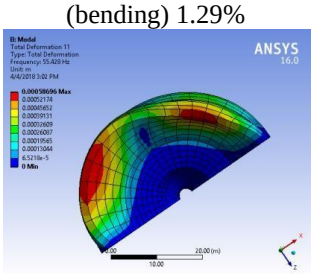

(k) Mode 11 (4th mode of lateral DOF) 56.647 Hz (torsion) 1.4%

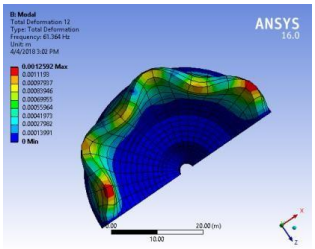

(l) Mode 12 (4th mode of torsional DOF) 61.116 Hz (bending and torsion) 1.05%

Fig. 8. Mode shape and frequency for concrete arch-gravity dam without soil foundation

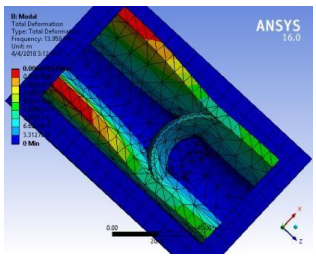

(a) Mode 1 (1st mode of longitudinal DOF) 12.899 Hz (displacement) 1.08%

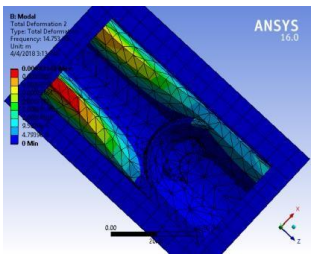

(b) Mode 2 (1st mode of lateral DOF) 14.705 Hz (displacement) 1.63%

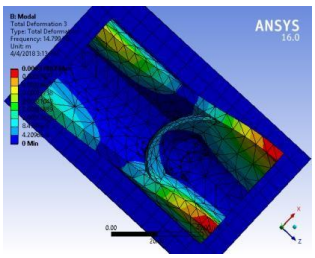

(c) Mode 3 (1st mode of torsional DOF) 16.126 Hz (torsion) 1.13%

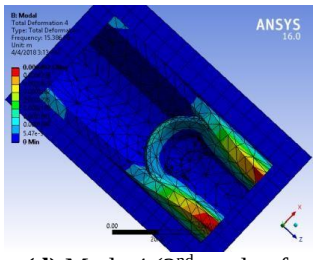

(d) Mode 4 (2nd mode of longitudinal DOF) 20.522 Hz (displacement) 1.26%

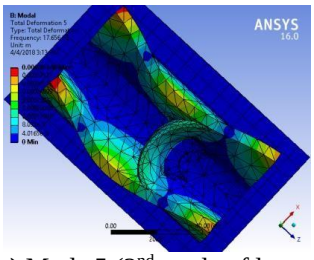

(e) Mode 5 (2nd mode of lateral DOF) 21.654 Hz (bending and torsion) 1.24%

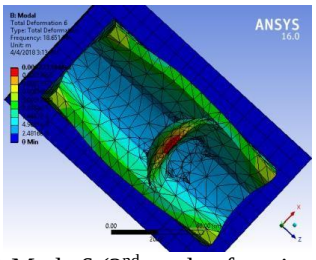

(f) Mode 6 (2nd mode of torsional DOF) 24.991 Hz (displacement) 1.61%

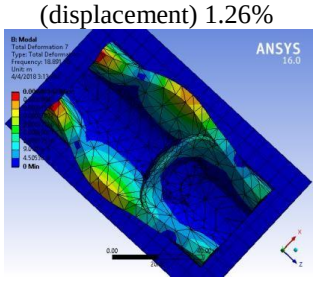

(g) Mode 7 (3rd mode of lateral DOF) 25.371 Hz (bending) 1.33%

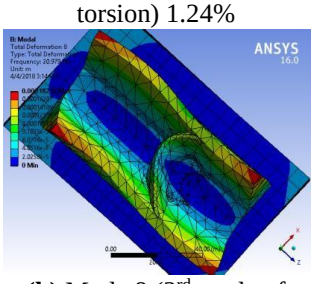

(h) Mode 8 (3rd mode of longitudinal DOF) 27.073 Hz (bending) 1.29%

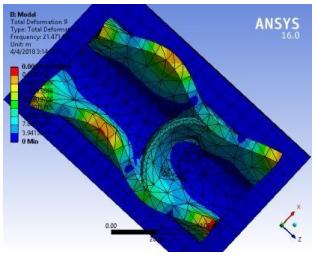

(i) Mode 9 (3rd mode of torsional DOF) 27.521 Hz (torsion) 1.74%

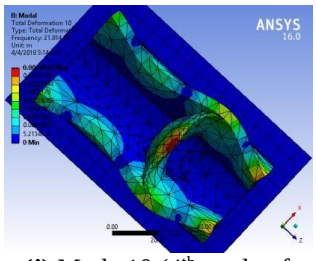

(j) Mode 10 (4th mode of longitudinal DOF) 28.838 Hz (bending) 1.20%

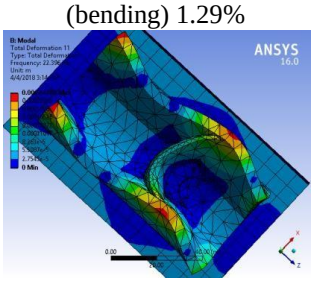

(k) Mode 11 (4th mode of lateral DOF) 29.275 Hz (torsion) 1.4%

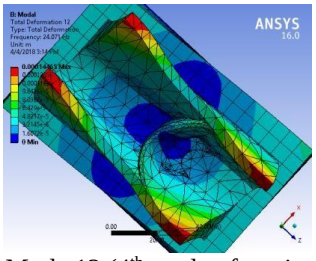

(l) Mode 12 (4th mode of torsional DOF) 29.275 Hz (bending and torsion) 1.05%

Fig. 9. Mode shape and frequency for concrete arch-gravity dam without soil foundation

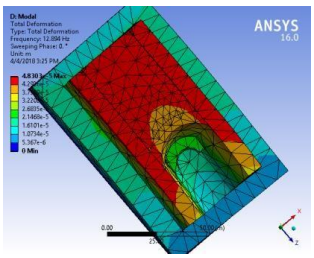

(a) Mode 1 (1st mode of longitudinal DOF) 7.572 Hz (displacement) 1.08%

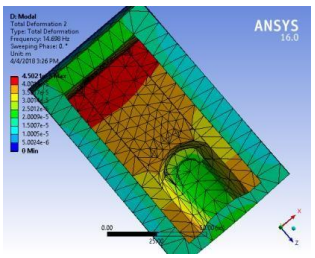

(b) Mode 2 (1st mode of lateral DOF) 8.665 Hz (displacement) 1.63%

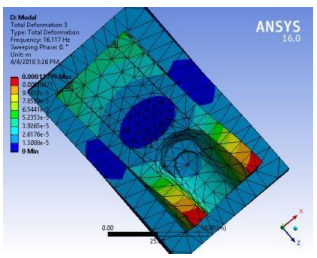

(c) Mode 3 (1st mode of torsional DOF)9.191 Hz (torsion) 1.13%

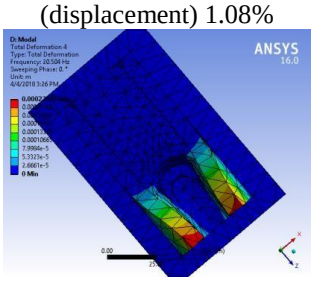

(d) Mode 4 (2nd mode of longitudinal DOF) 12.301 Hz (displacement) 1.26%

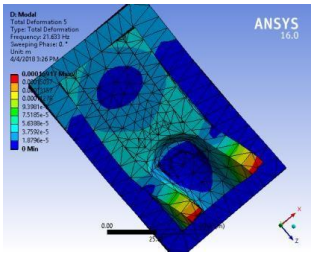

(e) Mode 5 (2nd mode of lateral DOF)13.025 Hz (Bending and torsion) 1.24%

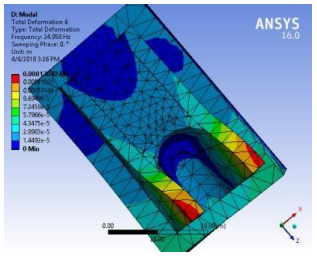

(f) Mode 6 (2nd mode of torsional DOF)13.073 Hz (displacement) 1.61%

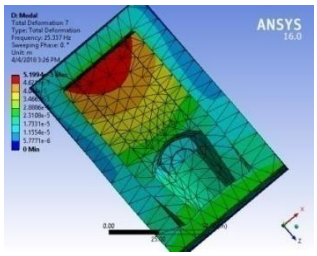

(g) Mode 7 (3rd mode of lateral DOF) 13.363 Hz (bending) 1.33%

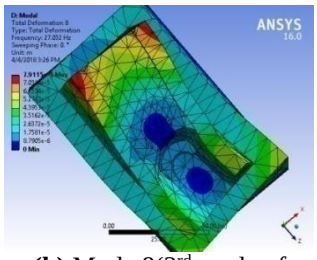

(h) Mode 8(3rd mode of longitudinal DOF) 14.144 Hz (bending) 1.29%

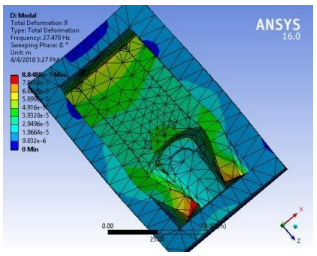

(i) Mode 9(3rd mode of torsional DOF) 14.994 Hz (torsion) 1.74%

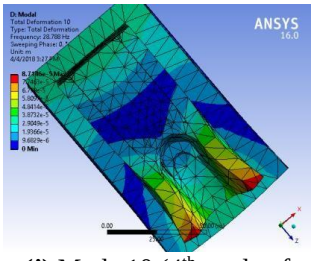

(j) Mode 10 (4th mode of longitudinal DOF) 16.215 Hz (bending) 1.20%

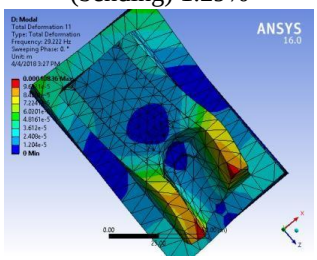

(k) Mode 11 (4th mode of lateral DOF)16.474 Hz (torsion) 1.4%

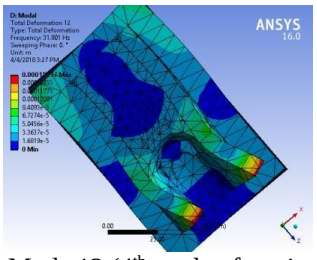

(l) Mode 12 (4th mode of torsional DOF) 16.96 Hz (bending and torsion) 1.05%

Fig. 10. Mode shape and frequency for concrete arch-gravity dam with soil foundation and reservoir

3.1.2.1. Mesh Convergence Study for Validation Model

The mesh size is a critical factor in the finite element analysis of any structure. For optimal outcomes, it is imperative to select an appropriate mesh size for each component. Mesh convergence is utilized in research to obtain more accurate and detailed information about the free vibration responses of buildings. The study was conducted to analyze fluctuations in the quantity of elements. The model was resolved by decreasing the mesh size and analyzing the results to observe the variations in accordance with the mesh size.

The process of meshing in ANSYS (2019) involves finding a balance between accuracy and computational cost when applying it to any structural model. A crucial aspect of creating an accurate simulation is the development of a top-notch mesh. In this section of the research, mesh convergence is performed to accurately determine the natural frequency of several types of concrete arch-gravity dams. Figure 11 displays the free vibration response for various mesh sizes. The simulation for the structure model in this work is performed using a mesh size of 200 mm, as determined by mesh convergence.

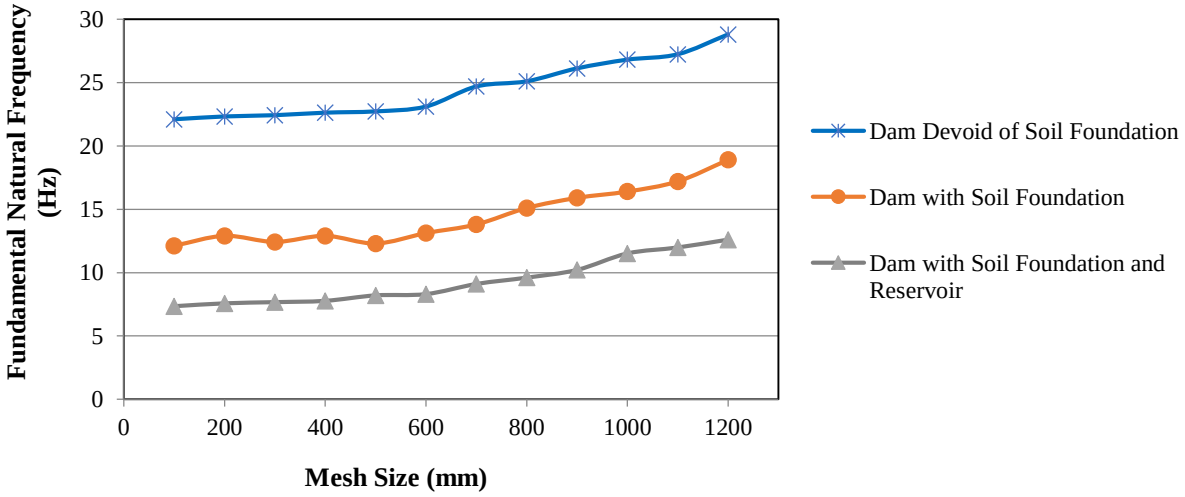

Fig. 11. Mesh convergence study

3.1.3. Parametric Study on Concrete Arch-Gravity Dam System

An analysis is conducted on the FEM model of a concrete arch-gravity dam to identify the several parameters that affect its modal properties. The current study has analyzed multiple parameters and provides a comprehensive explanation of the influence of each parameter.

- Influence of mass participation factor:

The number of simulated modes is contingent upon the vibration of various frequencies. According to the Indian standard code "IS 1893 (Part I)", the analysis should evaluate a number of modes that will result in about 90 percent of the modal mass being aroused. Therefore, based on the aforementioned statement, a total of 12 modes are derived from the arch dam, each having distinct configurations. Figure 12 displays the mode forms and associated free vibration frequencies for 30 modes of the dam under three different conditions: without a soil foundation, with a soil foundation, and with a soil foundation and reservoir. The primary mode exhibits a significant mass attendance in the x direction (76%), whereas its effective mass participation is in the y direction (35%). The top five modes constitute 86% of the overall mass participation, so establishing them as the most significant modes. The relationship between effective mass and total mass is almost similar in the x direction and is greater than that in the y and z directions, as seen in the Appendix (Tables A1-A2).

- Influence of Model Case:

Figure 12 displays the mode forms and associated free vibration frequencies for 30 modes of the dam in three different scenarios: without a soil basis, with a soil foundation, and with both soil and a reservoir.

The modal analysis results indicate that the dam's natural frequency is most prominent in Model 1, which represents a fixed-empty condition of the reservoir and soil foundation. Moreover, when dam-reservoir-soil foundation interaction is recognized (mass-fluid model), the most negligible value for the fundamental frequency is obtained, i.e., there is a 21% decrease in modal frequency for the first fundamental mode as well as more than 30-50% reduction in modal frequencies of all other higher modes if dam structure without soil foundation and dam structure with foundation is considered.

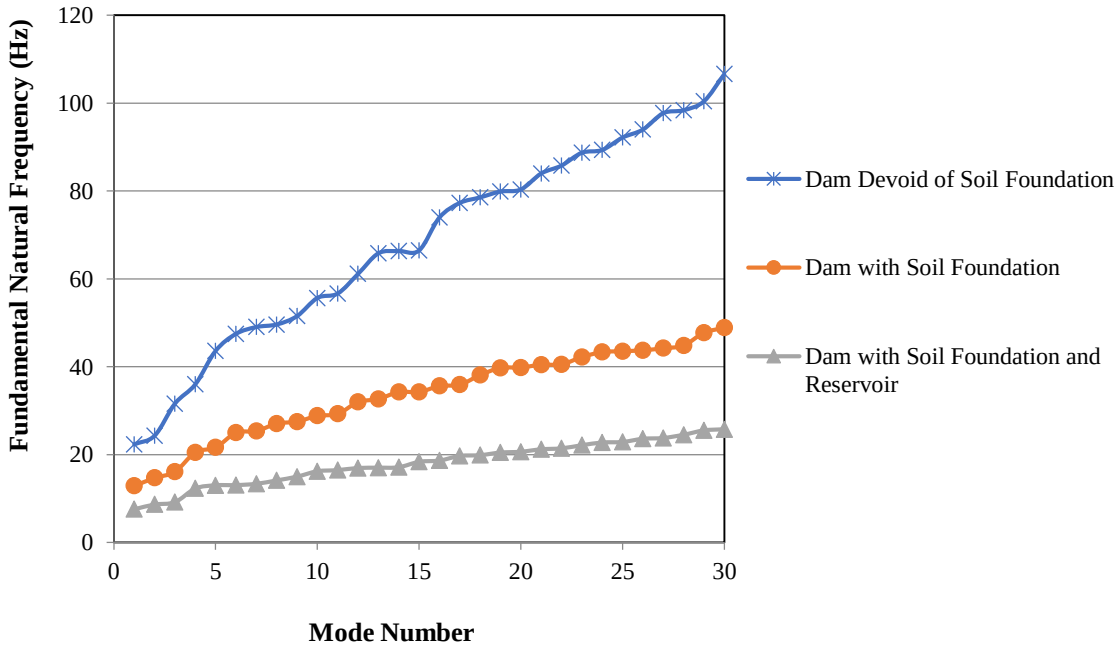

Fig. 12. Frequency of different modes for undamped free vibration

If dam structures with soil foundations and dam structures with soil foundation reservoirs are examined, the modal frequency of the first mode will be reduced by 12%, and the modal frequencies of the subsequent higher modes will be reduced by more than 15%.

When the structure foundation and structure reservoir are taken into account, the modal frequency of the first mode reduces by 22%, while the modal frequencies of other higher modes reduce by more than 51%. This is because when reservoir interaction is taken into account, the water surrounding the structure induces an increase in the inertial force operating on the structure. The hydrodynamic pressure acts on the structure as even the reservoir moves along with the displaced structure. Consequently, the presence of water in the reservoir affects the dynamic characteristics of the system by altering the patterns of motion and decreasing the frequency of vibrations.

Considering the influence of foundation interaction, the natural frequency of the dam is determined to be lower compared to a dam with fixed support. This is attributed to a reduction in stiffness and an increase in the mass of the vibrating system.

- Influence of Damping Ratio:

Furthermore, a computational analysis was conducted to examine the effects of viscous damping using the Rayleigh form. Figures 12-15 illustrate the mode forms and corresponding free vibration frequencies for 30 modes of undamped and damped systems with different damping ratios (ξ = 0, 2%, 5%, 10%).

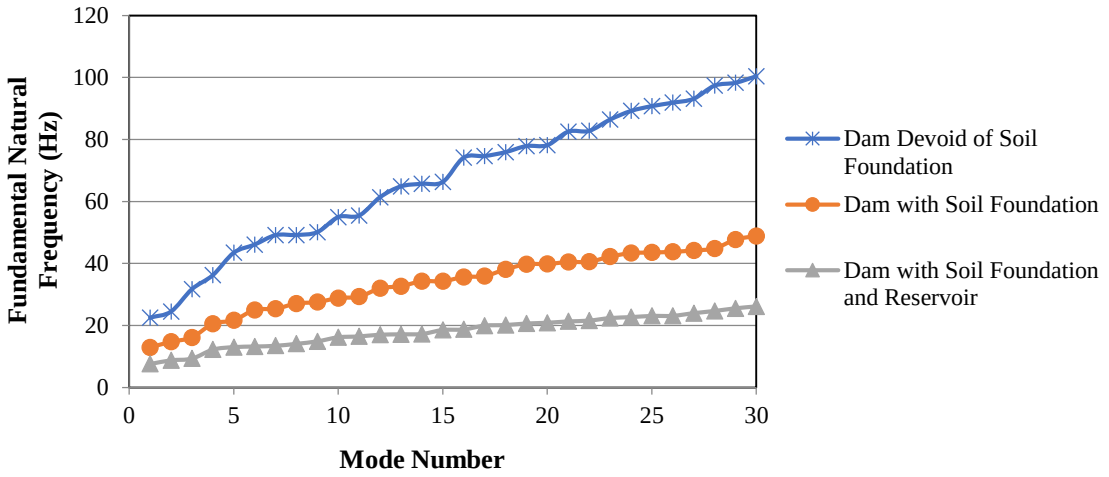

Fig. 13. Frequency of different modes for damped vibration (ξ = 2%)

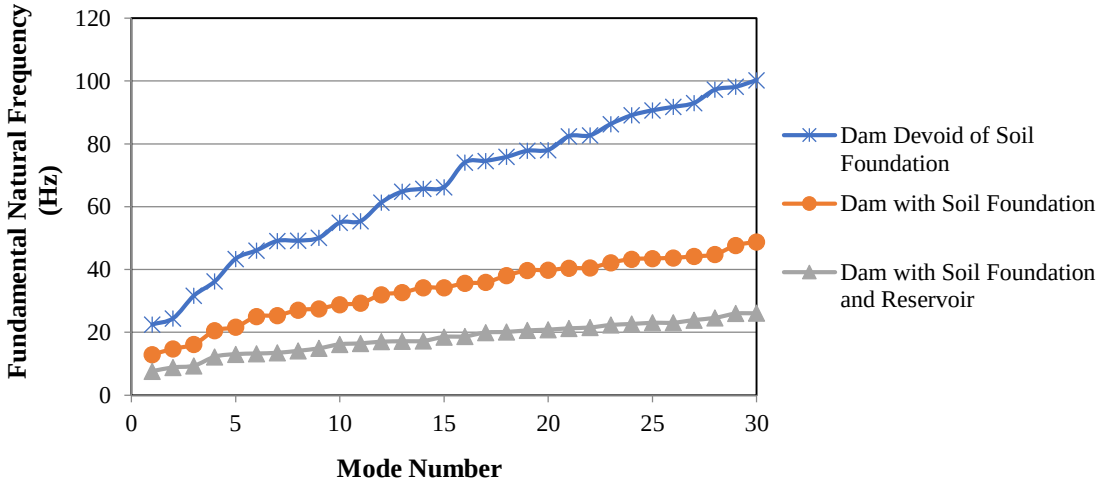

Fig. 14. Frequency of different modes for damped vibration (ξ =5%)

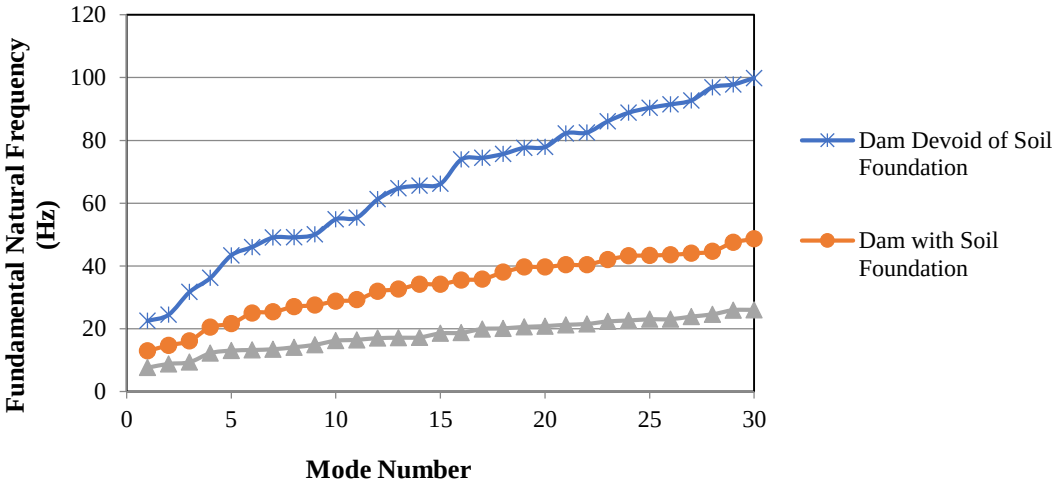

Fig. 15. Frequency of different modes for damped vibration (ξ =10%)

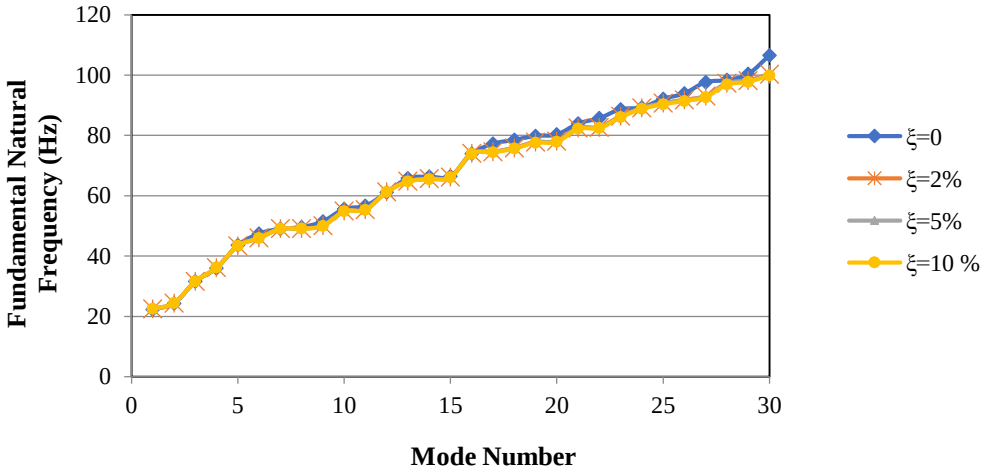

Fig. 16. Dam without a soil foundation

The systems include dams without a soil basis, dams with a soil foundation, and dams with a soil foundation plus a reservoir. Figures 17-18 demonstrate that the frequency (in Hertz) of undamped free vibration is almost indistinguishable from that of damped (0%, 2%, 5%, and 10%) vibration for all arch dam models.

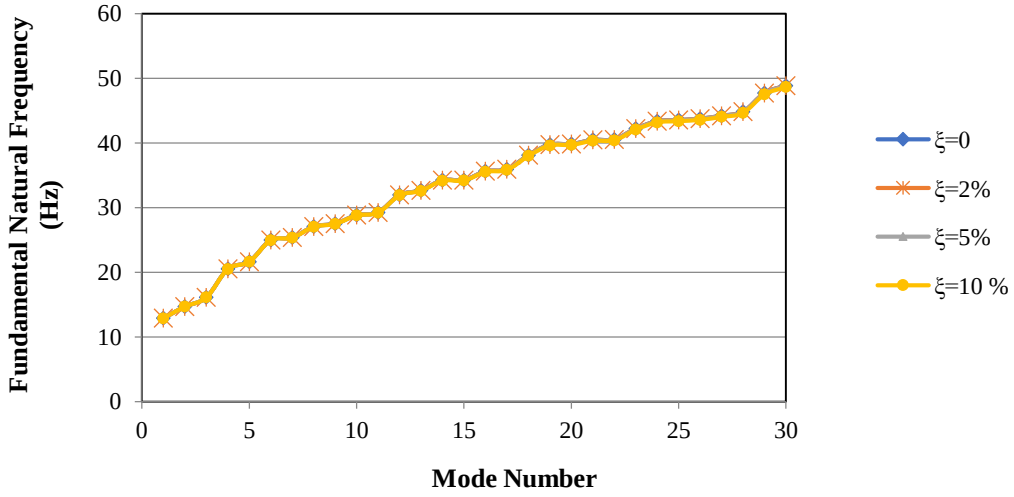

Fig. 17. Dam with soil foundation

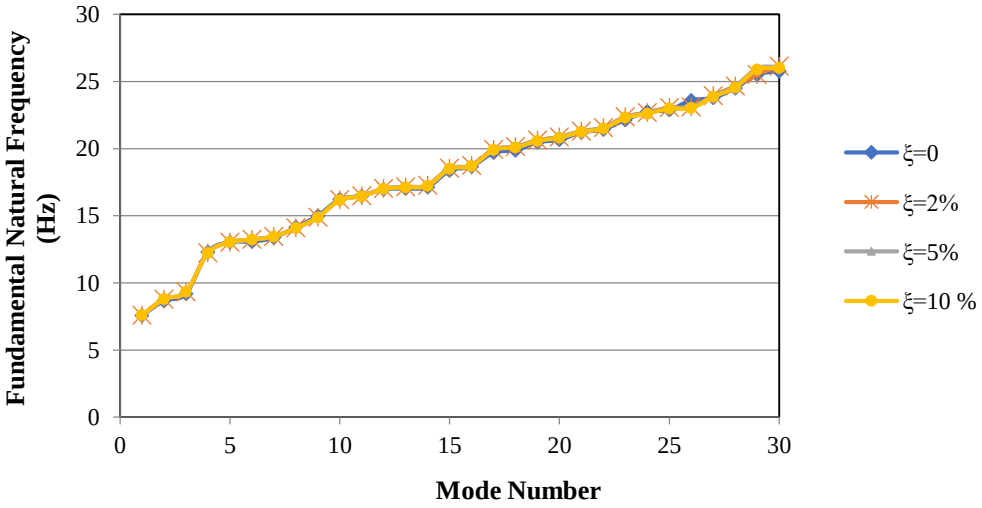

Fig. 18. Dam with soil foundation and reservoir

4. Conclusions

The current work has demonstrated the free vibration behavior of many dam models, including a dam without a soil basis, a dam with a soil foundation, a dam with soil, and a reservoir, using the 3D finite element program ANSYS. The discovered results will facilitate the more accurate design of dams, hence providing substantial advantages to society. The conclusion derived from the comprehensive analyses is succinctly summarized as follows:

The research concludes that the frequency of dams without soil contact is greater than that of dams with soil interaction and dams with both soil and reservoir. It can be described as a dam without a soil basis, a dam with a soil foundation, and a dam with both soil and a reservoir that have the same total mass. However, a dam that includes soil and a reservoir has a lower water stiffness.

Additionally, a dam with a soil foundation is somewhat less rigid due to the fact that the Young's modulus of soil is approximately half the value of a dam without a soil foundation. Consequently, this model is used to replicate lower frequencies. An exploration of the damping has also been conducted using parametric methods. The natural frequencies of both undamped and damped modes obtained from all arch dam models exhibit a high degree of similarity, with variations of only 2%, 5%, or 10%.

5. References

Abdollahi, A., Amini, A. and Hariri-Ardebili, M.A. (2022). "An uncertainty-aware dynamic shape optimization framework: Gravity dam design", *Reliability Engineering and System Safety*, 222, 108402, https://doi.org/10.1016/j.ress.2022.108402.

Altunişik, A.C., Günaydin, M., Sevim, B., Bayraktar, A. and Adanur, S. (2016). "Dynamic characteristics of an arch dam model before and after strengthening with consideration of reservoir water", *Journal of Performance of Constructed Facilities*, 30(6), 06016001, https://doi.org/10.1061/(ASCE)CF.1943-5509.0000890.

Amini, A., Abdollahi, A., Hariri-Ardebili, M.A. and Lall, U. (2021). "Copula-based reliability and sensitivity analysis of ageing dams: Adaptive kriging and polynomial chaos kriging methods", *Applied Soft Computing*, 109, 107524, https://doi.org/10.1016/j.asoc.2021.107524.

ANSYS (2019). *Ansys user's manual*, SAS IP Inc., Southpointe.

Berrabah, A.T., Belharizi, M., Laulusa, A. and Bekkouche, A. (2012). "Three-dimensional modal analysis of brezina concrete arch dam", *Algeria Earth Science Research*, 1(2), 55-70, https://doi.org/10.5539/esr.v1n2p55.

Borino, G. and Muscolino, G. (1986). "Mode-superposition methods in dynamic analysis of classically and non-classically damped linear systems", *Earthquake engineering and structural dynamics*, 14(5), 705-717, https://doi.org/10.1016/j.engstruct.2014.11.011.

Chopra, A.K. (2007). *Dynamics of structures*,

Pearson Education India.

Clough, R.W. and Penzien, J. (1995). *Dynamics of structures*, Computers and Structures, New York.

Esmaielzadeh, S., Ahmadi, H. and Hosseini, S.A. (2019). "A survey of matlab efficiency in damage detection of concrete gravity in concrete gravity dams", *IIUM Engineering Journal*, 20(1), 29-48, https://doi.org/10.31436/iiumej.v20i1.970.

Hashempour, S. A., Akbari, R. and Lotfi, V. (2023). "A simplified continuum damage model for nonlinear seismic analysis of concrete arch dams using different damping algorithms", *Civil Engineering Infrastructures Journal*, 56(2), 235-255, https://doi.org/10.22059/CEIJ.2023.342419.1837.

Heshmati, M., Hariri, A.M., Seyed, K.S. and Mirzabozorg, H. (2013). "Are there any differences in seismic performance evaluation criteria for concrete arch dams?", *Civil Engineering Infrastructures Journal*, 46(2), 233-240, https://doi.org/10.7508/ceij.2013.02.010.

Hariri-Ardebili, M.A., Seyed-Kolbadi, S.M. and Kianoush, M.R. (2016). "FEM-based parametric analysis of a typical gravity dam considering input excitation mechanism", *Soil Dynamics and Earthquake Engineering*, 84, 22-43, https://doi.org/10.1016/j.soildyn.2016.01.013.

Hariri-Ardebili, M.A., Mahdavi, G., Abdollahi, A. and Amini, A. (2021). "An rf-pce hybrid surrogate model for sensitivity analysis of dams", *Water*, 13(3), 302, https://doi.org/10.3390/w13030302.

Khosravi, S. and Heydari, M.M. (2015). "Design and modal analysis of gravity dams by ansys parametric design language", *Walailak Journal of Science and Technology (WJST)*, 12(2), 167-180, http:/doi.org/10.2004/wjst.v11i12.866.

Li, Z.Y., Hu, Z.Q., Lin, G. and Li, J.B. (2022). "A scaled boundary finite element method procedure for arch dam-water-foundation rock interaction in complex layered half-space", *Computers and Geotechnics*, 141, 104524, https://doi.org/10.1016/j.compgeo.2021.104524.

Messaad, M., Bourezane, M., Latrache, M., Berrabah, A.T. and Ouzendja, D. (2021). "Three-dimensional seismic analysis of concrete gravity dams considering foundation flexibility", *Mechanics and Mechanical Engineering*, 25(1), 88-98, http:/doi.org/10.2478/mme-2021-0012.

Pandey, A.D., Das, R., Mahesh, M.J., Anvesh, S. and Saini, P. (2016). "Structural analysis of a historical dam", *Procedia Engineering*, 144, 140-147, https://doi.org/10.1016/j.proeng.2016.05.017.

Patil, S.V. and Awari, U.R. (2015). "Effect of soil structure interaction on gravity dam", *International Journal of Modern Trends in Engineering and Research*, 2(7), 2349-9745,

Rasa, A.Y. and Budak, A. (2021). "Static and dynamic investigation of structure-foundation-reservoir problem utilizing finite element method", In: *Transactions of International Congress on the Phenomenological Aspects of Civil Engineering* (PACE-2021), 1-6.

Rasa, A.Y., Budak, A. and Düzgün, O.A. (2024a). "Seismic performance evaluation of concrete gravity dams using an efficient finite element model", *Journal of Vibration Engineering and Technologies*, 12(2), 2595-2614, https://doi.org/10.21203/rs.3.rs-2361487/v1.

Rasa, A.Y., Budak, A. and Düzgün, O.A. (2024b). "Concrete ageing effect on the dynamic response of machine foundations considering-Structure Interaction", *Journal of Vibration Engineering and Technologies*, 12(3), 3417-3429, https://doi.org/10.1007/s42417-023-01055-8.

Rasa, A.Y., Budak, A. and Düzgün, O.A. (2024c). "Concrete deterioration effects on the dynamic behavior of gravity dam-reservoir interaction problems", *Journal of Vibration Engineering and Technologies*, 12(1), 259-278, https://doi.org/10.1007/s42417-022-00842-z.

Rasa, A.Y., Budak, A. and Düzgün, O.A. (2024d). "The influence of concrete degradation on seismic performance of gravity dams", *Earthquakes and Structures*, 26(1), 59, https://doi.org/10.12989/eas.2024.26.1.059.

Rezaiee-Pajand, M., Sadegh Kazemiyan, M. and Mirjalili, Z. (2023). "A novel method for modal analysis of dam-reservoir systems", *Civil Engineering Infrastructures Journal*, 57(1), 33-59, https://doi.org/10.22059/CEIJ.2023.349505.1873.

Sharma, A. and Nallasivam, K. (2023). "Static analysis of a concrete gravity dam using the finite element technique", *Asian Journal of Civil Engineering*, 24(8), 2939-2957, https://doi.org/10.1007/s42107-023-00686-2.

Standard, IS. (1893). *Criteria for earthquake resistant design of structures*, Bureau of Indian Standards, Part 1.

Tickoo, S. (2021). *ANSYS workbench 2021 R1: A tutorial approach*, Purdue University and CADCIM Technologies.

Tavakoli, H., Mofid, T. and Dehestani, M. (2023). "Dynamic analysis of thermal crack propagation in roller-compacted Concrete dams considering rotational component of ground motion", *Civil Engineering Infrastructures Journal*, 57(2), 287-302, https://doi.org/10.22059/CEIJ.2023.361667.19

35.
Varughese, J.A. and Nikithan, S. (2016). "Seismic behaviour of concrete gravity dams", *Advances in Computational Design*, 1(2), 195-206, https://doi.org/10.12989/acd.2016.1.2.195.
Verma, V. and Nallasivam, K. (2020). "One-dimensional finite element analysis of thin-walled box-girder bridge", *Innovative Infrastructure Solutions*, 5, 1-24, https://doi.org/10.1007/s41062-020-00287-x.
Verma, V. and Nallasivam, K. (2021a). "Free vibration behaviour of thin-walled concrete box-girder bridge using Perspex sheet experimental model", *Journal of Achievements in Materials and Manufacturing Engineering*, 106(2), 56-76, https://doi.org/10.5604/01.3001.0015.2418.
Verma, V. and Nallasivam, K. (2021b). "Static response of curved steel thin-walled box-girder bridge subjected to Indian railway loading", *Journal of Achievements in Materials and Manufacturing Engineering*, 108(2), 63-74, https://doi.org/10.5604/01.3001.0015.2418.
Yaghin, M.A. and Hesari, M.A. (2008). "Dynamic analysis of the arch concrete dam under earthquake force with ABAQUS", *Journal of Applied Sciences*, 8(15), 2648-2658, https://doi.org/10.3923/jas.2008.2648.2658.
Zhang, X.Z., Sun, X.N. and Tang, K.D. (2013). "Static and dynamic analysis of concrete gravity dam by ANSYS", *Applied Mechanics and Materials*, 438, 1334-1337, https://www.scientific.net/AMM.438-439.1334.
Zhuan-Yun, Y. (2014). "Static and dynamic analysis of high arch dam by three-dimensional finite element method", *Electronic Journal of Geotechnical Engineering*, 19, 2537-2551.

6. Abbreviations

2D: Two Dimensional,
3D: Three Dimensional,
ABAQUS: Finite Element Method software,
ANSYS: Analysis System,
DOEA: Disregard of Off-diagonal Elements in the non-classical damping matrix,
DOF: Degree of Freedom,
DR: Damping Ratio,
DRFI: Dam-Reservoir-Foundation Interaction,
DRI: Dam-Reservoir Interaction,
DFI: Dam-Foundation Interaction,
FEM: Finite Element Method,
FORTRAN 90: Programming Language,
IS: Indian Standard,
MATLAB: Matrix Laboratory,
PCE: Polynomial Chaos Expansion surrogate model,
RF: Random Field,
SAP 2000: Structural Analysis and Design,
SBFEM: Scaled Boundary Finite Element Method,
UQ: Uncertainty Quantification.

7. Appendix

Tables A1-A2 show the participation factor calculation in the dam's *x*, *y*, and *z* directions without and with soil interaction.

Table A1. Participation factor (without soil interaction)

Mode	Frequency in Hz	Time period in sec	Partic. factor	Ratio	Effective mass	Cumulative mass fraction	The ratio of eff. mass to the total mass
			x- x direction				
1	22.323	0.4e-01	-0.4e-03	0.000	0.20e-06	0.122e-13	0.765e-14
5	43.609	0.2e-01	-0.1e-02	0.001	0.22e-05	0.765e-01	0.860e-13
15	66.458	0.1e-01	1093.0	0.491	0.12e+07	0.944	0.452e-01
25	92.152	0.1e-01	-761.23	0.342	579465	0.989	0.219e-01
30	106.568	0.9e-01	-318.85	0.143	101668	1.000	0.384e-02
			y-y direction				
1	22.323	0.4e-01	0.3e-02	0.001	0.93e-05	0.5085e-12	0.352e-12
5	43.609	0.2e-01	-0.1e-02	0.000	0.12e-05	0.383	0.468e-13
15	66.458	0.1e-01	919.76	0.401	845966	0.835	0.320e-01
25	92.152	0.1e-01	-321.53	0.140	103382	0.982	0.391e-02
30	106.568	0.9e-01	-298.90	0.130	89339.9	1.000	0.338e-02
			z-z the direction				
1	22.323	0.4e-01	0.3e-02	0.001	0.93e-05	0.5085e-12	0.352e-12
5	43.609	0.2e-01	-0.1e-02	0.000	0.12e-05	0.383	0.468e-13
15	66.458	0.1e-01	919.76	0.401	845966	0.835	0.320e-01
25	92.152	0.1e-01	-321.53	0.140	103382	0.982	0.391e-02
30	106.568	0.9e-01	-298.90	0.130	89339.9	1.000	0.338e-02

Table A2. Participation factor calculation in *y*- *y* direction (with soil interaction)

Mode	Frequency in Hz	Time period in sec	Partic. factor	Ratio	Effective mass	Cumulative mass fraction	The ratio of eff. mass to the total mass
			x- *x* direction				
1	7.572	0.13206	20490	1.000	0.42e+09	0.737	0.589
5	13.025	0.7e-01	5118.3	0.249	0.26e+08	0.7843	0.368e-01
15	18.366	0.5e-01	-332.26	0.016	110400	0.997	0.155e-03
25	22.879	0.4e-01	622.41	0.030	387393	0.999	0.544e-03
30	25.768	0.3e-01	-204.53	0.009	41333.2	1.000	0.597e-04
			y-*y* direction *x*- *x* direction				
1	7.57	0.13206	53.096	0.002	2819.15	0.568e-05	0.396e-05
5	13.025	0.7e-01	832.88	0.042	693684	0.224e-01	0.974e-03
15	18.366	0.5e-01	13.328	0.001	177.625	0.885	0.249e-06
25	22.879	0.4e-01	-137.68	0.006	18956.0	0.989	0.266e-04
30	25.768	0.3e-01	-908.44	0.045	825264	1.000	0.115e-02
			z-*z* the direction				
1	7.572	0.13206	-1.1196	0.001	1.25354	0.211e-08	0.176e-08
5	13.025	0.7e-01	429.20	0.019	184215	0.843	0.258e-03
15	18.366	0.5e-01	215.87	0.009	46600.4	0.944	0.654e-04
25	22.879	0.4e-01	13.964	0.001	195.00	0.999	0.273e-06
30	25.768	0.3e-01	-500.25	0.022	250248	1.0000	0.351e-03